20 Years SAR Interferometry for Monitoring Ground Deformation over the former Potash-Mine "Glückauf" in Thuringia.

Clémence Dubois, Jannik Jänichen, Marco Wolsza,
Nesrin Salepci & Christiane Schmullius

Geophysical processes and anthropogenic activities cause the deformation of the Earth's surface, both mechanisms interacting sometimes simultaneously. While the occurrence of those processes in rural areas may not always directly affect the population, the determination of surface deformation in inhabited areas is of high relevance to prevent risks. Traditional surveying techniques provide exact but usually spatially and temporally limited deformation information, making a regular monitoring of whole urban areas difficult. Since about 20 years, RADAR remote sensing, especially SAR interferometry, provide dense and accurate ground motion information, completing hereby the traditional monitoring techniques. This present study investigates ground surface dynamics in a town close to a former potash-mine situated in the northern part of Thuringia, Germany, by means of multi-temporal SAR interferometry. Using the method of Persistent Scatterer Interferometry, 20 years of RADAR data from multiple sensors are evaluated and compared to in-situ data. It shows that ground subsidences decreased since the closing and backfilling of the mine, which is in accordance with surveying activities on this site.

1. Introduction

The monitoring of the Earth's surface and its deformation is of high relevance for many environmental applications. The aim is, in particular, to gain a better understanding of the geological and geophysical processes and of the impact of anthropogenic activities on these processes. Among the possible applications, risk prevention through infrastructure and ground deformation monitoring plays an important role. The use of RADAR remote sensing technology is constantly gaining in importance in this field. Especially, through the increasing number of RADAR satellites and freely available data, new opportunities for large scale time-series analysis of such data arise. Through regular visit time and large spatial coverage, these sensors represent an attractive complement to traditional surveying techniques. One specific application of those sensors is the detection of ground motion in the order of a few millimeters a year through multitemporal differential SAR interferometry. Two principal methods have been developed in the early 2000s for this purpose: Persistent Scatterer Interferometry (PSI) (Ferretti, A. 2001) and Small-Baseline Subset (SBAS) (Berardino, P. et al 2002).

doi.org/10.15488/9339

They have been used since for a broad range of deformation monitoring applications. Considering the analysis of synergistic effects of anthropogenic activities and geophysical processes, the principal applications include the monitoring of geothermal facilities (Lubitz, C. et al. 2012), landslides (Casagli, N. et al. 2016), groundwater (over)exploitation due to intensive irrigation (Alipour, S. et al. 2008) but also the monitoring of infrastructure stability such as buildings (Gernhardt, S. 2011) or the determination of the stress exerted on gas-pipelines built on different foundations (Ianoschi, R. et al. 2013). Finally, those interferometric methods are increasingly used for the monitoring of oil and gas extraction (Gee, D. et al. 2016) as well as mining and back-filling activities (Salepci 2015, Racoules et al. 2003, Walter et al. 2009, Perski et al. 2009, Samsonov et al. 2013). Mining activities can cause land subsidence through the extraction of underground material. If the mining area is situated close to cities, the consequences can be disastrous for the houses situated above – from small cracks in the facades to larger damages (Ilieva, M. et al. 2019). Being able to monitor the subsidence and the effect of possible counter-measures – e.g. backfilling of the mine shaft- can help prevent the risk of building collapsing and resulting social disagreement.
In most cases and depending on the availability of the sensors data, PSI analysis is conducted with data from a single sensor over a limited period of time. (Crosetto, M. et al. 2016) reports a few approaches using datasets from at least two sensors for monitoring of infrastructures and mines for longer period of times. Usually data from sensors having the same characteristics, e.g. C-Band, are combined (Herrera, G. et al. 2007). In this study, we combine data from four different sensors (three C-band and one L-band) in order to observe deformations over a former salt-mine in northern Thuringia for a period of twenty years using Persistent Scatterer Interferometry. We present the study area and datasets in Section 2. Section 3 summarizes the principal parameters of the applied approach for deformation estimation. In Section 4, we present the results for the different datasets and combine the displacement rates for the total observation period.

2. Study area and data

2.1. Study area

The study area is a former potash-mine, situated in the northern part of Thuringia, Germany. The mine entrance is situated in the north western part of the city of Sondershausen (pop. 25000), and northeast of the town of Großfurra (pop. 1500). The considered area for analysis encompasses therefore both towns of Sondershausen and Großfurra. Figure 1a represents the geographic location of the study area as well as the delineation of the potash-mine "Glückauf". It shows that part of the mine is directly situated underneath the city of Sondershausen.
The "Glückauf" mine is situated in the Thuringian Basin, a depression bordered to the north by the Harz mountains and to the south by the Thuringian Forest. The basin's geological setting is characterised by almost horizontal bedding of sedimentary rocks, the

largest deposits being red sandstone, shell limestone and Keuper from Triassic. Gypsum and salt are found below this bedding sequence, dating from middle to late Permian (Seidel, G. 2003). The geological columnar section of the stratigraphic sequence at the study area is given in Figure 1b.
The spatial distribution of the mined minerals of the potash-mine "Glückauf" is represented in Figure 1a. Mainly potash salt such as carnallite and sylvine have been mined, as well as rock salt such as halite (Fliss, T. et al. 2011). A total of 110 millions tons of salt has been extracted between 1898 and 1991 from the "Glückauf" mine, in depths varying from 600m to 1000m over an area of approximately 60km² (TLUG 2005). Intensive mining giving rise to an increasing instability of the mine, and uneconomical production since the early 1970s led to the termination of the production and the closing of the mine in 1991 (Zschiedrich, K. et al. 2017).

Figure 1: a) geographical location of the study area and spatial distribution of extracted minerals (modified from Zschiedrich, K. et al. 2017) ; b) Stratigraphy of the study area (Salepci 2015)

At the time of closing, subsidences up to 25cm/year were measured at the surface above the mining area, and many seismic events were recorded (up to magnitude 1.8 on the Richter scale) (Fliss, T. et al. 2011). Such subsidence rates can cause significant damage to buildings and infrastructures situated in the area (Zschiedrich, K. et al. 2017). Backfilling measures have been taken between 1991 and 1997 (Zschiedrich, K. et al. 2017), consisting of filling the cavities with rock salt excavated from a different part of the mine (Marx, H. et al. 2005). Those actions brought quick results and led to a decrease in the amount and magnitude of seismic events, as well as a decelerating subsidence rate over the mining area (Fliss, T. et al. 2011). Figure 2 shows the subsidence rates in the city center of Sondershausen between 1980 and 2015. We notice an increase of the subsidence from 1985 to the closing of the mine in 1991, followed by a rapid decrease of the subsidence rates from 1991 to 1998, and a lower but continuous decrease of the subsidence since.

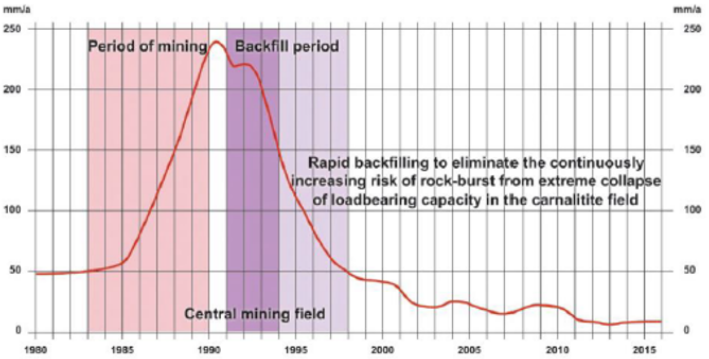

Figure 2: Subsidence rates in the city center of Sondershausen between 1980 and 2015 (Zschiedrich, K. et al. 2017)

The mine reopened in 1996 for touristic activities and concerts, and in 2006, halite mining started again for the production of road salt.

2.2. Satellite Data

In this study, we considered 20 years of SAR data for monitoring subsidence in the area of the mine "Glückauf". As operational SAR sensors providing a sufficient amount of acquisitions for monitoring purposes only started in the early 1990s, we considered data from 1995 to 2019 from four different satellite sensors, having a gap of only four years during this period of time. Table 1 resumes the considered sensors and respective acquisition parameters.

Table 1: Considered satellite data and acquisition parameters

Sensor	Band	Spatial Resolution (ra x az)	Start of acquisitions	End of acquisitions	Revisit time	Number of acquisitions	Incidence angle over study area	Orbit
ERS-1/2	C-Band	30 x 30 m	08.04.1995	23.10.2005	35 days	74	23°	Desc.
Envisat-ASAR	C-Band	28 x 28 m	11.04.2004	12.09.2010	35 days	21	23°	Desc.
ALOS-PALSAR	L-Band	19 x 10 m	02.03.2007	26.07.2010	46 days	15	38°	Asc.
Sentinel-1A	C-Band	5 x 20 m	10.2014	04.2019	12 days	55	34°	Desc.

Data from the sensors ERS-1/2, Envisat-ASAR, ALOS-PALSAR and Sentinel-1 were considered. A graph of the temporal baseline versus geometrical baseline for each sensor is

given in Section 3, Figure 5.
The ERS-1/2 dataset shows a higher density of acquisitions in the years before 2000. Due to several consecutive failures of the on-board gyroscopes of ERS-2 occurring in early 2000, the Doppler Centroid (DC) frequency was affected (Miranda, N. et al. 2003). Passed a certain DC shift, decorrelation between affected acquisitions and earlier acquisitions is too high in order to be used for interferometry, resulting in larger time gaps between suitable acquisitions for interferometric analysis since 2000. Whereas before the year 2000 the maximum temporal baseline was of 70 days, it was of 525 days after 2000.
The Envisat-ASAR dataset shows a more regular distribution of the acquisitions over time, with larger gaps between 2006 and 2009.
The ALOS-PALSAR dataset contains only 15 datasets acquired between 2007 and 2010. The number of acquisitions corresponds to the minimal required for Persistent Scatterer Interferometry (Ferretti, A. 2004), resulting in a possibly slightly worse accuracy of the displacement estimates than for the other sensors. The considered acquisitions were acquired regularly, the maximal perpendicular baseline being slightly larger than for the other sensors. However, as ALOS PALSAR works in L-Band, the perpendicular baseline can be larger without geometric decorrelation occurring. Due to the longer wavelength of ALOS PALSAR compared to the other C-Band sensors, the signal path/penetration on the objects of the Earth surface may differ, e.g. L-Band can penetrate up to the forest ground where C-Band would be scattered back by the upper branches of a forest canopy. However, as the considered area principally consists of buildings and man-made infrastructures, similar backscatter centers are expected for all sensors, with a possible higher number of detected persistent scatterers (PS) of L-Band as it can penetrate vegetated areas up to more stable scatterers than leaves, e.g. tree trunk, and due in this case to the finer resolution than the considered C-Band sensors.
In order to keep the computation time low, the Sentinel-1 datasets considers only acquisitions of Sentinel-1A. The data stack contains 55 datasets, acquired very regularly on a 12 days revisit time.

2.3. Auxiliary Data

Four different kinds of auxiliary data were used for processing and validation of the results. A LIDAR DEM of 5 m resolution was provided by the Thuringian Institute for Environment, Mining and Nature Conservation (Thüringer Landesamt für Umwelt, Bergbau und Naturschutz -TLUBN). It is used during processing for the coregistration of the SAR acquisitions, for the calculation of the differential interferograms and for geocoding.
For supporting the selection of the master scene for PSI processing, weather data from the German Meteorological Service (Deutscher Wetterdienst -DWD) were considered. In particular, information about atmospheric pressure, air temperature, relative and absolute humidity, cloud coverage, snow height and precipitation were used at each acquisition time for making a rough estimation of atmospheric water vapor in order to distinguish scenes more or less affected by atmospheric effects. In this study, data from the weather station Artern, situated approximately 20 km in the East of Sondershausen, were used.
Finally, for the validation of the estimated displacement rates, surveying data from a

network of 137 leveling points is taken into account. This network has been measured every year between 1995 and 2011 and measurements are provided with 1mm accuracy by the Glückauf mine management companies GSES mbH (Glückauf Sondershausen Entwicklungs- und Sicherungsgesellschaft) and GVV mbH. The deformations monitored for each individual point have been pre-processed in order to estimate a linear displacement and averaged subsidence rate for the different epochs of the satellite observations. It results in a homogeneous and similar representation as for the PS points, for better comparison. A representation of the levelling points and their vertical estimated velocities for the different periods of satellite acquisitions is given in Figure 3.

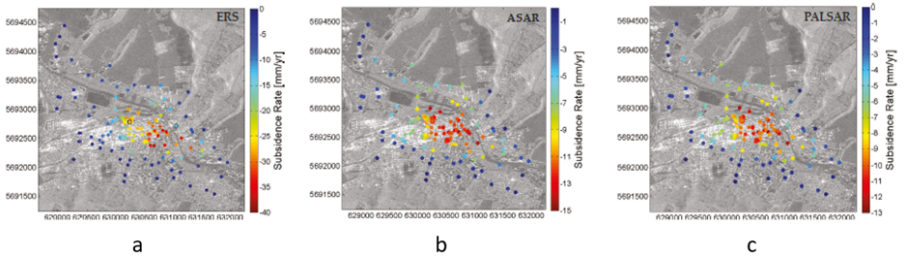

Figure 3: Subsidence observed during levelling campaigns during the period a) 1995-2005, b)2004-2010 and c) 2007-2010 (Salepci 2015)

For the period 2014-2019 (Sentinel-1), no levelling information was available. Instead, information from the National Ground Motion Service of Germany (BodenBewegungsdienst Deutschland - BBD, BGR 2019) were used. The BBD Service provides ground motion information calculated using Persistent Scatterer Interferometry on Sentinel-1 data between 2014 and 2018 in ascending direction. Whilst not directly comparable with the results of the presented approach due to different period of observations and acquisition direction, the data and subsidence rates for specific areas can be used in order to roughly validate the observed displacements. These data will be shown in Section 4.

3. Methods

The PSI processing has been performed using the GAMMA Software, based on the PSI method presented in (Ferretti, A. 2001). A workflow showing the principal steps is presented in Figure 4 and specific parameter setting and considerations are resumed in the following.

For each sensor, the considered data stack has been processed separately. The calculated velocities and displacements are therefore calculated for each dataset independently on the respectively extracted persistent scatterers.
For all considered datasets, a pre-processing of the Single Look Complex (SLC) data was conducted using precise orbit files when available, in order to obtain accurate orbit state

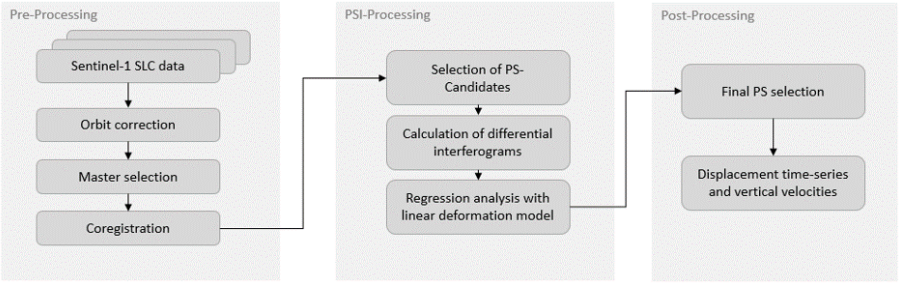

Figure 4: Processing workflow - Principal steps

vectors and ease the coregistration process. The selection of the optimal master scene for each data stack happened under consideration of both temporal and perpendicular baseline. Additionally, weather conditions were analysed at the dates of all acquisitions in order to rank the acquisitions depending on the influence of atmospheric disturbances. The final master scene for each data stack was chosen as the scene presenting optimal temporal and perpendicular baselines with the other scenes and few atmospheric influence (Salepci 2015). A representation of the temporal and perpendicular baselines for each sensor and acquisition considered for the interferometric analysis is given in Figure 5. The selected master scene is represented in Figure 5 for each data stack in red.

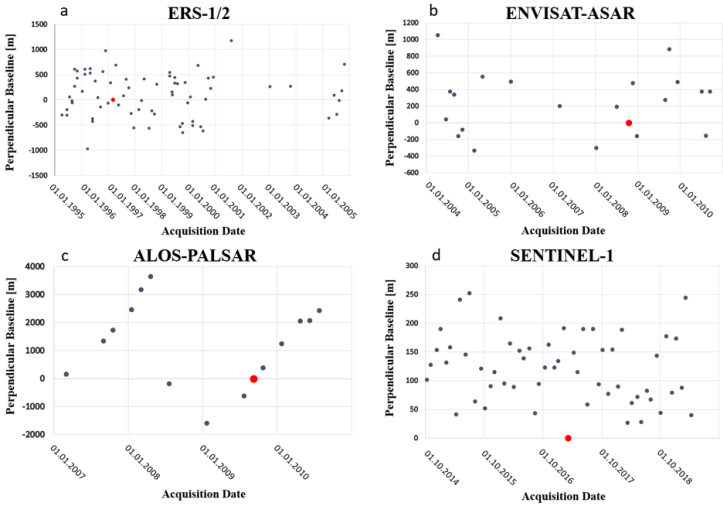

Figure 5: Connection Graph: perpendicular and temporal baselines of the considered acquisitions w.r.t the selected master scene (red dot) for a) ERS-1/2, b) ENVISAT-ASAR, c) ALOS-PALSAR and d) Sentinel-1.

The coregistration of the slave scenes with the master scene was improved using the LIDAR DEM in order to better consider offset caused by stronger topography. After subsetting the images, PS candidates were selected using both the Amplitude Dispersion Index and the Spectral Phase Diversity, which selects pixels with high temporal stability of the backscatter values and low variation of the power spectrum, respectively. The differential interferograms are calculated in the next steps and subsequently a two dimensional regression analysis is performed on the phase values, considering spatial and temporal phase differences. To this purpose, a reference point is chosen which displacement rate is known or assumed to be stable over time. The calculated velocities and displacements are all relative to this point. Lacking any GPS data, the reference point was chosen in a stable area, where no large deformation was expected, so that the estimated deformations correspond approximately to absolute deformations. The displacements were estimated using a linear deformation model, i.e. only PS candidates showing linear displacement over time will be retained as PS points at the end of the analysis.
Post-processing was applied on all data stacks as shown in (Salepci, N. 2015). Furthermore, Line-of-Sight (LOS) displacements were converted into vertical displacements, assuming that the horizontal displacements over mining areas are negligible and the observed LOS displacements are a projection of the vertical displacements into the LOS (similar to Walter, D. et al. 2009 and Perski, Z. et al. 2009). In this case, the conversion of the displacements is straightforward, using the local incidence angle:

$$v_u = \frac{v_{LOS}}{cos\theta},$$

v_u being the vertical velocity, v_{LOS} the velocity on LOS direction and θ the incidence angle.

4. Results and Discussion

Table 2 resumes for each data stack the number of final PS points found and retained in the study area, as well as the mean uncertainty of the estimated deformation rate in mm/yr.

Table 2: Overview of the selected number of PS candidates and of final PS after post-processing

Sensor	Number of PS Candidates	Number of final PS	Mean deformation rate uncertainty [mm/yr]
ERS-1/2	2795	1465	0.2
ENVISAT-ASAR	3119	1527	0.3
ALOS-PALSAR	12842	4436	2.2
SENTINEL-1	16257	7029	0.2

It is observable that about half or less of the original number of PS candidates is retained after processing. Despite the larger data gaps during the observation period of ERS-1/2, a sufficient number of PS points has been detected and can be analysed. ALOS-PALSAR and Sentinel-1 show both a higher number of PS, probably due for both to the higher resolution and the shorter observation time - with a high number of acquisitions for Sentinel-1 - where it is expected that less scatterers may change as during longer observation periods.

Figure 6 shows for all data stacks the corresponding estimated velocity maps. It is observable for all time periods and data stacks that two particular areas show high ground motion compared to their stable surroundings: the city center of Sondershausen in the middle-east of the figures, and part of the town of Großfurra in the north-western part of the figures. Having a look at Figure 1a, it is obvious that those subsidences occur over areas that have been mined for salt, the upper left parts of Figure 1a corresponding to mixed-salt mining under the town of Großfurra.

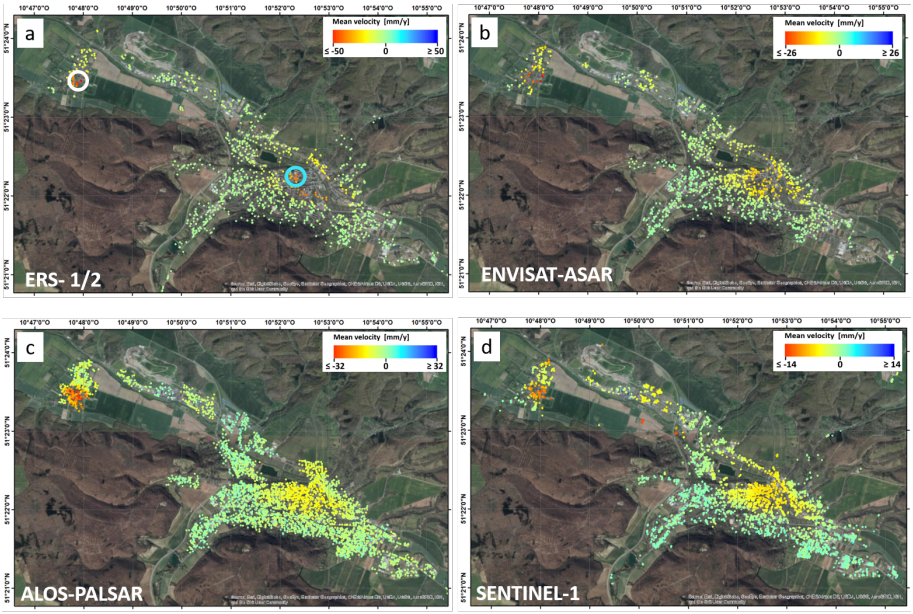

Figure 6: Maps of the estimated mean vertical velocity in the study areas for the different periods of observation: a) ERS-1/2 from 1995-2005, b) ENVISAT-ASAR from 2004-2010, c) ALOS-PALSAR from 2007-2010 and d) Sentinel-1 from 2014-2019. (Source of underlying optical imagery: ESRI, DigitalGlobe, GeoEye, Earthstar Geographics, CNESAirbus DS, USDA, USGS, AeroGRID, IGN and the GIS User Community).

In general, we can observe the decreasing of the subsidence rates over the whole observation period. Whereas the subsidence rates in the years after the closing of the mine were up to -51mm/yr, the subsidence seems to diminish in the mid-2000s, the highest subsidence rate detected in the area by the ENVISAT-ASAR processing being of -26mm/yr and by ALOS-PALSAR of -34mm/yr. The newest processing of the Sentinel-1 data shows further reduction of the subsidence rates to a maximum of -11mm/yr in the city of Großfurra. Table 3 shows for both areas encircled in white (Großfurra) and blue (Sondershausen) lines in Figure 6a the mean and maximum velocity values for the different data stacks. Those areas correspond to the city parts of Sondershausen and Großfurra showing the higher subsidence rates. Here also, it is visible that the subsidences decrease during the observation period, showing the positive effects of the back-filling of the mine shafts. ENVISAT-ASAR and ALOS-PALSAR show small differences of the observed deformations rates, ALOS-PALSAR showing in general higher deformation rates as ENVISAT-ASAR, although the data have been acquired later. ALOS-PALSAR also shows higher uncertainties of the estimated deformation rates than the other sensors (Table 2). This is probably due to the shorter period of observation for ALOS-PALSAR and the lower number of acquisitions. Further observation of the sensor specific parameters (Table 1) indicates that the data from ALOS-PALSAR have been acquired with different acquisition frequency, spatial resolution and orbit direction compared to the other sensors, which leads to different observed scatterers. Due to the direction of acquisitions, the detected PSs in the city are probably different from the detected PSs of the other sensors, as they may be situated on the other sides of buildings, facing the sensor. The original LOS, from which the vertical velocities have been calculated, is also different, which may cause the slightly different subsidence rate observed between ENVISAT-ASAR and ALOS-PALSAR. The different incidence angles considered by the different sensors may lead to different detected PSs, and cause further differences between the observed deformations. However, as all observations have been conducted at different periods of time, with the deformation rates expecting to change in between, the analysis of the specific influence of the incidence angle on the observed deformation is not feasible.

Table 3: Averaged and maximum observed velocities for the two cities situated in the study area

Sensor	Subsidence rate Großfurra (white circle) mean / max [mm/yr]	Subsidence rate Sondershausen (blue circle) mean / max [mm/yr]
ERS-1/2	-31 / -51	-34 / -39
ENVISAT-ASAR	-14 / -26	-11 / -12
ALOS-PALSAR	-18 / -34	-11 / -15
Sentinel-1	-8 / -13	-6 / -9

ERS-1/2 and ENVISAT-PALSAR show very similar acquisition parameters, so that the observed differences are only due to the deformation. Sentinel-1 shows a higher incidence

angle, which may lead to the detection of different scatterers. However the influence of the considered incidence angle on the estimated deformation is considered negligible, as the ground motion is the same for all scatterers situated in a specific area, and it is assumed that there is no other deformation cause in this area and all scatterers move similarly to the ground.

Figure 7 shows for the blue circle shown in Figure 6a (city of Sondershausen) the mean time-series displacement of the area over the years, assuming linear displacement between the period of observations. It should be noticed that the number of PS for averaging differs for the different observation periods. Here also, the reduction of the subsidence rates is well observable. Especially since the early 2000s, the accumulated displacements increase at a lower rate. A high correlation exists between the cumulated displacements calculated for ENVISAT-ASAR and for ALOS-PALSAR. Very high displacements are observed for ERS-1/2 at the end of the acquisition period. This is probably due to the longer temporal baseline between the acquisitions, leading to uncertainties in the displacement calculation. Furthermore, the fitted deformation model assumes linearity of the displacements over time, which may not correspond to reality, as different kinds of motion can occur on different objects and the overall subsidence rates my diminish over time through backfilling activities. The higher deviation from the linearity observed for the ERS-1/2 acquisitions in the early 2000s could therefore be due to a reduction of the motion velocity around these years, which is observable for both ENVISAT-ASAR and ALOS-PALSAR. This could also explain the lack of detected PSs for ERS-1/2 in the city center (eastern side of the blue circle in Figure 6a), as most of the motion in this area may have undergone a different, non-linear, deformation model.

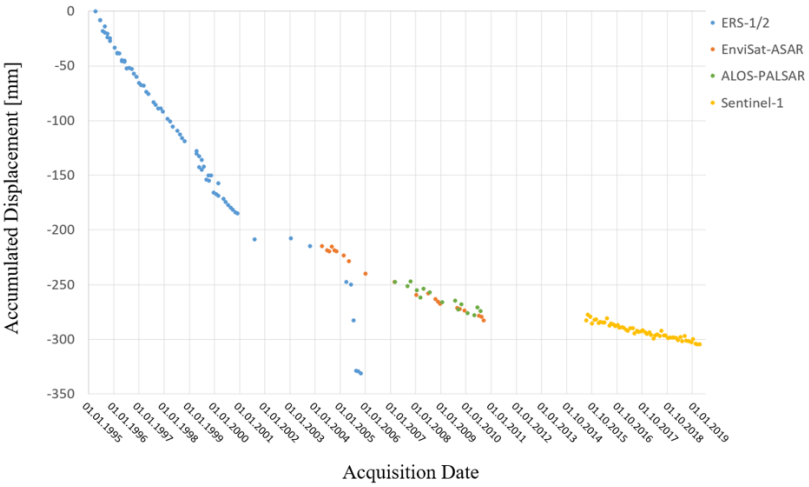

Figure 7: Observed accumulated displacements for the 20 years of observation, averaged within the blue circle shown in Figure 6a.

A comparison with the levelling data is only possible for the three earlier data stacks and for the city center of Sondershausen. A direct comparison is not possible, as the geolocation of levelling points are well known (usually situated on metallic bolts fixed in house walls or sidewalks) but the geolocation of the PS points can only be estimated within a perimeter corresponding to the resolution of the data. In order to validate those results, we considered for each levelling point the mean subsidence rates of all PS points situated within different radii and averaged, as described in (Salepci, N. 2015). The radii were defined for each dataset in order to optimize the number of PSs present within the area without risking changing the displacement regime. Figure 8 shows for the three data stack of ERS-1/2, ENVISAT-ASAR and ALOS-PALSAR scatter plots of the mean PS subsidence rates and the levelling points, with corresponding correlation coefficient (ρ). The colors represent the number of PS points situated within the defined radii for each levelling point. A good concordance between observed deformation rates with PS Interferometry and levelling data is noticeable.

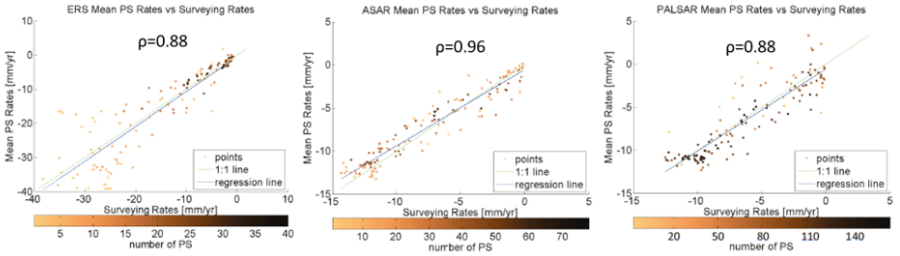

Figure 8: Comparison of the observed subsidence rates for a) ERS-1/2, b) ENVISAT-PALSAR and c) ALOS-PALSAR with the levelling data (modified after Salepci, N. 2015)

Due to missing levelling data, the validation of the observed deformations during the period of observation of Sentinel-1 stack has been performed using an independent PSI-Analysis performed in the framework of the German Ground Motion Service (BodenBewegungsdienst Deutschland - BBD, BGR 2019). It is important to mention here the principal differences between the calculated dataset and the validation dataset. The BBD uses Sentinel-1 data acquired between 2014 and 2018 in an ascending path, i.e. the compared period of observation overlap but do not match exactly. Furthermore, for the BBD, both Sentinel-1A and -1B were used, providing more datasets, whereas in our approach, only data from Sentinel-1A were considered in order to keep the computation time low. In our approach, we used descending orbits paths, whereas ascending paths were used for the BBD. It involves that the detected PSs, even though situated in similar areas, do not obligatory correspond to the same points on the surface. Furthermore, the deformations from BBD is shown in Line-of-Sight (LOS) whereas we transformed the observed LOS into vertical deformations (see section 3). Despite those differences and assuming that most of the deformations occurring in our case are of vertical nature, similar deformation patterns can permit a rough validation of our results. Figure 9 shows both our results

and the corresponding area from the BBD. Similar patterns and deformation rates are observable for our study area: the town of Großfurra shows in the North and South the highest deformation rates, whereas the town center is more stable. Moreover, the city center of Sondershausen shows maximum deformation rate in ascending LOS for the BBD of -9mm/yr, at which approximated location we observe in vertical direction subsidence rates of about -8mm/yr. The general estimated deformation rates and patterns of both products concur, allowing a coarse validation of results.

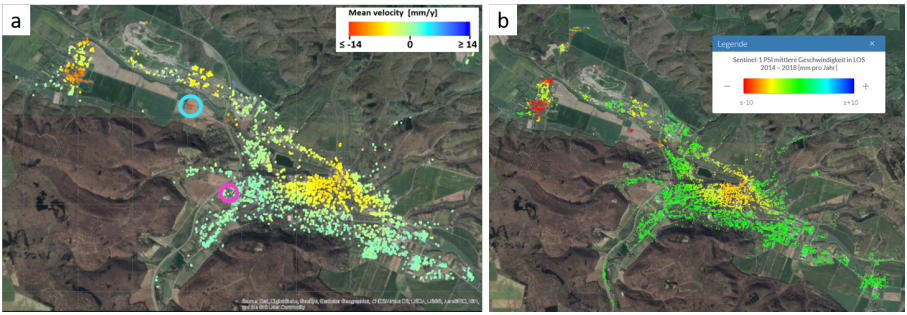

Figure 9: a) mean vertical velocities estimated in our approach for the Sentinel-1 time- period b) mean LOS velocities estimated in the framework of the BBD (BGR 2019)

It is also interesting to notice that some scattered points in the area between both cities show for Sentinel-1 high subsidence rates in both our and the BBD products, whereas they were stable in earlier years (ERS-1/2). Those points are encircled in blue lines in Figure 9. A closer look on optical imagery indicates the presence of a power plant and power poles in its surrounding, at least since the early 2000s. Further analysis of the influence of thermal dilation and dielectric properties on the estimated displacement would be needed to better understand the observed deformation.

Finally, even on stable area, the displacement profile of certain PS points shows recurring pattern over time (Figure 10). Especially, the temporal variations show a yearly cycle with uplift during winter and subsidence during summer. Different causes exist for the occurrence of seasonal effects in PSI displacement profiles (Notti, D. et al. 2015, Gernhardt, S. 2010). This seemingly elastic deformation is observable for several points in an area where red sandstone is situated between the surface and the ancient salt mine-shaft (Seidel, G. 2003). In Thuringia, this material characterized by coarse grain size represents an essential element for ground water storage (Kunkel, C. 2016). An observation that could corroborate this hypothesis is that this regular up-and-down pattern (elastic deformation) seems to disappear during summer 2018, which was characterized by very dry conditions compared to the previous years. Further information about the geology would be needed in order to assess this hypothesis.

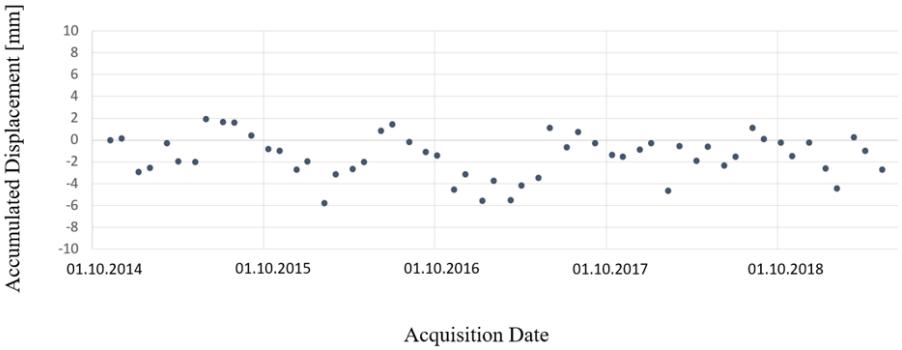

Figure 10: Displacement time-series of the point encircled in magenta in Figure 9 (situated in a stable area)

5. Conclusion

In this study, we have analysed data from four different sensors over a period of twenty years in order to monitor the subsidence rates after back-filling activities of the ancient potash-mine "Glückauf" of Sondershausen, in northern Thuringia. During the first years of backfilling activities, the subsidence was still high, with subsidence rates up to -51mm/yr observed with ERS-1/2. A reduction of the subsidence rates is observable with ENVISAT-ASAR and ALOS-PALSAR. The more recent analysis of Sentinel-1 data confirms this trend, with subsidence reaching a maximum of about -13mm/yr in the city center of Großfurra but an average of -6mm/yr in the city center of Sondershausen. The observations have been validated using levelling information and independent PSI analysis from the German Ground Motion Service. A detailed analysis of specific PS points show periodic displacements whose interpretation necessitates additional auxiliary data and will be object of future work. Especially, focus will be made on the analysis of different motion types. This analysis considered only linear motion, but the reality can be much more complex: non-linear deformation are more likely to happen over longer time-span, as the subsidence velocity may diminish with backfilling activities. Furthermore, depending on the geology, elastic deformations may occur that need to be analysed in further details.

Acknowledgements

The authors would like to thank the GSES mbH and the GVV mbH for providing the levelling data that were used for the validation of the observed subsidence rates between 1995 and 2010.

References

Alipour, S., Motgah, M., Sharifi, M. A., Walter, T. R. (2008): InSAR time series investigation of land subsidence due to groundwater overexploitation in Tehran, Iran. In 2008 Second Workshop on Use of Remote Sensing Techniques for Monitoring Volcanoes and Seismogenic Areas, pp. 1-5. doi: 10.1109/USEREST.2008.4740370.

Berardino, P., Fornaro, G., Lanari, R., Sansosti, E. (2002): A new algorithm for surface deformation monitoring based on small baseline differential SAR interferograms. IEEE Transactions on geoscience and remote sensing, 40(11), 2375-2383.

BGR (2019) : BodenBewegungsdienst Deutschland (BBD) https://bodenbewegungsdienst.bgr.de/mapapps/resources/apps/bbd/index.html?lang=de (last access: 09.12.2019)

Casagli, N., Cigna, F., Bianchini, S., Hölbling, D., Füreder, P., Righini, G., Del Conte, S., Schneiderbauer, C., Iasio, C., Vlcko, J., Greif, V., Proske, H., Granica, K., Falco, S., Lozzi, S., Mora, O., Arnaud, A., Novali, F., Bianchi, M. (2016): Landslide mapping and monitoring by using radar and optical remote sensing: Examples from the EC-FP7 project SAFER. Remote sensing applications: society and environment, 4, pp. 92-108.

Crosetto, M., Monserrat, O., Cuevas-González, M., Devanthéry, N., Crippa, B. (2016): Persistent scatterer interferometry: A review. ISPRS Journal of Photogrammetry and Remote Sensing, 115, 78-89.

Ferretti, A., Prati, C., Rocca, F. (2001): Permanent scatterers in SAR interferometry. IEEE Transactions on geoscience and remote sensing, 39(1), 8-20.

Ferretti, A. (2014): Satellite InSAR data: reservoir monitoring from space. EAGE publications.

Fliss, T., Marx, H., Thoma, H., Stäubert, A., Lindenau, A., D. Lack (2011): Backfilling and pillar re-mining in potash industry. In: Proceedings of MINEFILL 2011 - International Conference on Mining with Backfill, Cape Town, South Africa.

Gee, D., Sowter, A., Novellino, A., Marsh, S., Gluyas, J. (2016): Monitoring land motion due to natural gas extraction: Validation of the Intermittent SBAS (ISBAS) DInSAR algorithm over gas fields of North Holland, the Netherlands. Marine and Petroleum Geology, 77, 1338-1354.

Gernhardt, S., Adam, N., Eineder, M., Bamler, R. (2010): Potential of very high resolution SAR for persistent scatterer interferometry in urban areas. Annals of GIS, 16(2), 103-111.

Gernhardt, S. (2011): High precision 3D localization and motion analysis of persistent scatterers using meter-resolution radar satellite data. Doctoral dissertation, Technische Universität München.

Herrera, G., Tomás, R., López-Sánchez, J. M., Delgado, J., Mallorqui, J. J., Duque, S., Mulas, J. (2007): Advanced DInSAR analysis on mining areas: La Union case study (Murcia, SE Spain): Engineering Geology, 90(3-4), 148-159.

Ianoschi, R., Schouten, M., Leezenberg, P. B., Dheenathayalan, P., Hanssen, R. (2013): Satellite Radar Interferometry For Risk Management Of Gas Pipeline Networks. In ESA Living Planet Symposium, 722, pp. 60-63.

Ilieva, M., Polanin, P., Borkowski, A., Gruchlik, P., Smolak, K., Kowalski, A., Rohm, W. (2019): Mining Deformation Life Cycle in the Light of InSAR and Deformation Models. Remote Sensing, 11(7), 745.

Kunkel, C. (2016): Facies and aquifer characterization of the German triassic Buntsandstein in central Germany (Doctoral dissertation).

Lubitz, C., Motagh, M., Wetzel, H., Anderssohn, J. (2012): TerraSAR-X Time series uplift monitoring in Staufen, South-West Germany. 2012 IEEE International Geoscience and Remote Sensing Symposium, Munich, 2012, pp. 1306-1309. doi: 10.1109/IGARSS.2012.6351298.

Marx, H. et al. (2005): "Substantial aspects of the recycling of industrial wastes as backfilling material in salt mines". In: Proceedings of 20th World Mining Congress & Expo2005, Tehran, Iran, 7-11 November.

Miranda, N., B. Rosich, C. Santella, and M. Grion (2003): "Review of the impact of ERS-2 piloting modes on the SAR Doppler stability". In: Proceedings of FRINGE 2003 Workshop, Frascati, Italy, 1 – 5 December

Notti, D., Calo, F., Cigna, F., Manunta, M., Herrera, G., Berti, M., Meisina, C., Tapete, D., Zucca, F. (2015): A user-oriented methodology for DInSAR time series analysis and interpretation: Landslides and subsidence case studies. Pure and Applied Geophysics, 172(11), 3081-3105.

Perski, Z., Hanssen, R., Wojcik, A., Wojciechowski, T. (2009): InSAR analyses of terrain deformation near the Wieliczka Salt Mine, Poland. Engineering Geology, 106(1-2), 58-67.

Raucoules, D., C. Maisons, C. Carnec, S. Le Mouelic, C. King, and S. Hosford (2003): "Monitoring of slow ground deformation by ERS radar interferometry on the Vauvert salt mine (France), comparison with ground-based measurement". In: Remote Sensing of Environment 88, pp. 468–478.

Salepci, N. (2015): Multi-sensor synergy for persistent scatterer interferometry based ground subsidence monitoring. Doctoral Dissertation, urn:nbn:de:gbv:27-20150831-110916-8.

Samsonov, S., d'Oreye, N., Smets, B. (2013): Ground deformation associated with post-mining activity at the French–German border revealed by novel InSAR time series method. International Journal of Applied Earth Observation and Geoinformation, 23, 142-154.

Seidel, G. (2003): "Geologie von Thüringen". 2nd. Schweizerbart'sche Verlagsbuchhandlung, Stuttgart, Germany.

TLUG (2005): "Thüringen Untertage". Thüringer Landesanstalt für Umwelt und Geologie, Jena, Germany.

Walter, D., U. Wegmüller, Spreckels V., W. Hannemann, W. Busch (2009): "Interferometric monitoring of an active underground mining field with high-resolution SAR sensors". In: Proceedings of ISPRS Hannover Workshop 2009, WG I/2, I/4, IV/2, IV/3, VII/2, High-Resolution Earth Imaging for Geospatial Information, Hannover, Germany, 2 - 5 June.

Zschiedrich, K., Pietsch, T., Kuyumcu M (2017): Bewältigung von technischen, ökologischen und sozialen Herausforderungen bei der Stilllegung von Kalibergwerken in Ostdeutschland. Mining Report Glückauf 153, No. 3.

Contact

Clémence Dubois

Jannik Jänichen

Marco Wolsza

Nesrin Salepci

Christiane Schmullius

Department for Earth Observation
Institute of Geography
Friedrich-Schiller University Jena
Fürstengraben 1
07743 Jena
(clemence.dubois, jannik.jaenichen, marco.wolsza,
nesrin.salepci, c.schmullius)@uni-jena.de